

X-ray structure, hydrogen bonding and lattice energy analysis of (2*E*)-1-(anthracen-9-yl)-3-(4-substitutedphenyl)prop-2-en-1-ones

VINUTHA V SALIAN¹, B NARAYANA¹, K BYRAPPA¹, B K SAROJINI² and RAJNI KANT^{3,*}

¹Department of Studies in Chemistry, Mangalore University, Mangalagangothri 574 199, India

²Department of Studies in Chemistry—Industrial Chemistry Division, Mangalore University, Mangalagangothri 574 199, India

³X-ray Crystallography Laboratory, Post-Graduate Department of Physics and Electronics, University of Jammu, Jammu Tawi 180 006, India

MS received 17 March 2015; accepted 26 April 2016

Abstract. (2*E*)-1-(anthracen-9-yl)-3-(4-chlorophenyl)prop-2-en-1-ones and (2*E*)-1-(anthracen-9-yl)-3-(4-nitrophenyl)prop-2-en-1-ones crystallize in the monoclinic crystal system with space group P2₁/c. Single-crystal X-ray diffraction data for both the compounds were collected on an X²Calibur CCD area detector diffractometer (Oxford Diffraction) using MoK α radiation ($\lambda = 0.7107 \text{ \AA}$) at 293(2) K. The crystal structures were solved by direct methods and refined by full-matrix least-square procedures to a final *R* value of 0.0468 [I] and 0.0486 [II]. The crystal structures as elucidated by X-ray diffraction methods show the presence of a few intermolecular interactions, and the nature and energetics associated with these interactions have been characterized using PIXEL software.

Keywords. Anthracene; prop-2-en-1-one; crystal structure; intermolecular interactions; lattice energy; PIXEL.

1. Introduction

Chalcone is an aromatic ketone and an enone that forms a central core for a variety of pharmacologically important heterocyclic compounds. Chalcones are an important class of secondary metabolites that are precursors of many naturally occurring plant pigments [1]. These small molecules are also used as starting materials in the synthesis of UV absorption filters in polymers, photorefractive polymers, photosensitizers in colour films, sweeteners in food technology and in holographic recording technology. Chalcones, considered as the precursors of flavonoids and isoflavones, are also known to be effective antimicrobial agents [2].

Natural and synthetic chalcones have been attracting great interest owing to their broad range of biological activities, such as antileishmanial [3] anti-invasive [4], antitubercular [5], antifungal [6], antimalarial [7], anticancer [8] and anti-inflammatory activities [9]. They are biosynthetic precursors of triaryl pyridines [10], pyrazoles [11] and indazoles [12]. These α , β -unsaturated ketones were found to be effective photosensitive materials and exhibit potential nonlinear optical properties [13].

Chalcones are also known to possess antioxidant character to various extents. Activated macrophages play a key role in inflammatory responses and release a variety of mediators,

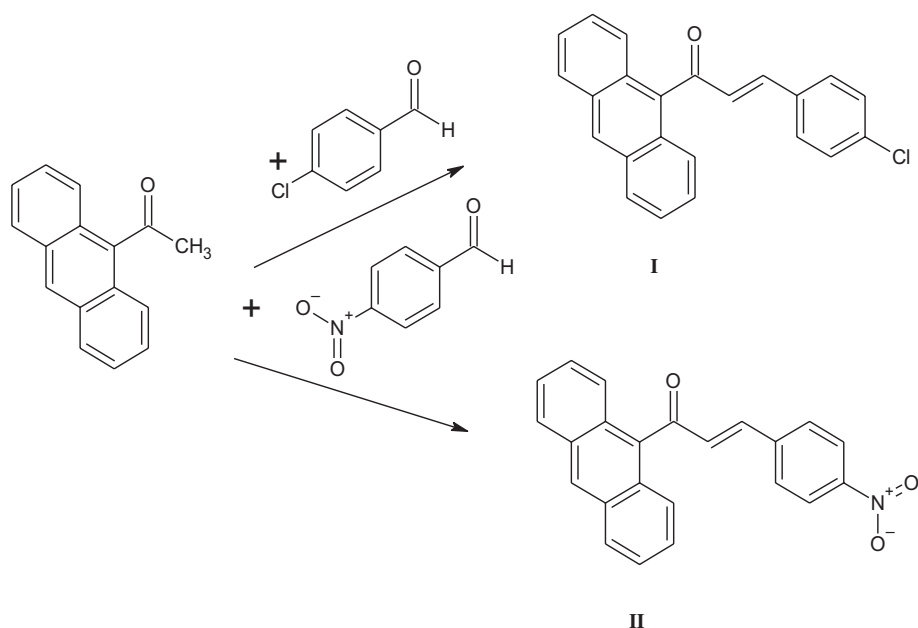
including nitric oxide (NO). NO is a potent vasodilator that facilitates leukocytic migration and formation of edema as well as leukocytic activity and cytokine production [2]. The crystal structures of some chalcone derivatives *viz.*, 2,3-dibromo-1,3-bis(4-fluorophenyl)propan-1-one [14], 3-(3,4-dimethoxyphenyl)-1-(4-fluorophenyl)prop-2-en-1-one, 2-bromo-1-(4-methylphenyl)-3-[4-(methylsulphonyl)phenyl]prop-2-en-1-one [15], (2*E*)-1-(4-chlorophenyl)-3-[4-(propan-2-yl)phenyl]prop-2-en-1-one [16] and 2-bromo-1-chlorophenyl-3-(4-methoxyphenyl)prop-2-en-1-one [17] have been reported. Keeping in view the wide range of activities of the chalcones, we report the crystal structure and lattice energy analysis of both the compounds.

2. Experimental

2.1 Synthesis and crystallization

To a mixture of 4-chlorobenzaldehyde (1.4 g, 0.01 mol) or 4-nitrobenzaldehyde (1.5 g, 0.01 mol) and 9-acetylanthracene (2.2 g, 0.01 mol) in ethanol (50 ml), 15 ml of 10% sodium hydroxide solution was added and stirred at 0–5°C for 3 h. The process of synthesis is depicted in the reaction scheme. The precipitate formed was collected by filtration and purified by recrystallization from ethanol. Single crystals of **I** and **II** were grown from ethanol by slow evaporation method (compound **I**: M.P. 429–431 K; compound **II**: M.P. 432–434 K).

* Author for correspondence (rkant.ju@gmail.com)



Reaction scheme for the title compounds.

2.2 Data collection and refinement details

Single-crystal X-ray diffraction data of both the compounds were collected on an *X'Calibur* CCD area detector diffractometer (Oxford Diffraction) using *MoKa* radiation ($\lambda = 0.7107 \text{ \AA}$) at 293(2) K [18]. The crystal structures were solved by direct methods using SHELXS97 [19] and full-matrix least-square structure refinement against F^2 was performed using SHELXL97 [19] software present in the program suite WinGX [20]. All the non-hydrogen atoms were refined anisotropically and all the hydrogen atoms were geometrically fixed and allowed to ride on their parent C atoms with C–H = 0.93 Å for both the compounds [$U_{\text{iso}}(\text{H}) = 1.2U_{\text{eq}}(\text{C})$]. Detailed crystallographic data for compounds **I** and **II** have been deposited at the Cambridge Crystallographic Data Centre (CCDC No. 1045455 for **I** and CCDC No. 1045454 for **II**) and are available on request. Crystal data collection parameters and structure refinement details for compounds **I** and **II** are summarized in table 1. Details of intermolecular hydrogen bonding for **I** and **II** are given in table 2 and π – π interaction geometry in table 3.

2.3 Computations

Geometrical calculations were performed using PLATON [21] and PARST [22] software. PIXEL calculations were performed in order to estimate the nature and energies associated with the intermolecular interactions, which will enable us to explore the role of these interactions in the stabilization of the crystal lattice. PIXELC calculations as incorporated in the Coulomb–London–Pauli (CLP) program [23] were performed to determine intermolecular interaction energies

and lattice energy. PIXEL calculations allow the analysis of lattice and intermolecular interaction energies between pairs of molecules in terms of coulombic, polarization, dispersion and repulsion contributions. The total PIXEL energy, which is the sum of these four energy contributions, gives an indication of the overall interaction energy for a particular dimer and for crystal packing. However, it is the separation of these energies into the four different terms that makes this method a powerful tool for crystal structure analysis.

3. Theoretical calculations

To get a better understanding of the contribution of intermolecular interactions to the crystal packing, it is important to get a quantitative evaluation of these interactions. Calculation of the lattice energy not only offers a possible way for polymorph prediction but may also help understand the supramolecular chemistry and self-assembly during the nucleation and crystal growth processes and helps predict the melting and solubility behaviour of the compounds. The lattice energy of the title compound was calculated by PIXELC module in CLP computer program package (version 13.2.2012) [23]. The total lattice energy is partitioned into its coulombic, polarization, dispersion and repulsion contributions. In CLP program, the coulombic terms are handled by Coulomb's law while the polarization terms are calculated in the linear dipole approximation, with the incoming electric field acting on local polarizabilities and generating a dipole with its associated dipole

Table 1. Experimental data for compounds **I** and **II**.

| | I | II |
|---|---|---|
| <i>Crystal data</i> | | |
| CCDC no. | 1045455 | 1045454 |
| Crystal description | White | White |
| Crystal size | 0.3 × 0.2 × 0.2 mm ³ | 0.3 × 0.2 × 0.2 mm ³ |
| Empirical formula | C ₂₃ H ₁₅ Cl ₁ O ₁ | C ₂₃ H ₁₅ N ₁ O ₃ |
| Formula weight | 342.80 | 353.36 |
| Radiation, wavelength | MoK α , 0.71073 Å | MoK α , 0.71073 Å |
| Unit cell dimensions | $a = 14.595(2)$ Å $b = 11.0790(8)$ Å $c = 11.435(2)$ Å $\beta = 112.98(2)^\circ$ | $a = 13.2972(13)$ Å $b = 12.6236(16)$ Å $c = 11.0415(11)$ Å $\beta = 105.667(9)^\circ$ |
| Crystal system | Monoclinic | Monoclinic |
| Space group | P2 ₁ /c | P2 ₁ /c |
| Unit cell volume | 1702.3(4) Å ³ | 1784.6(3) Å ³ |
| No. of molecules per unit cell, Z | 4 | 4 |
| Temperature | 293(2) K | 293(2) K |
| Absorption coefficient | 0.231 mm ⁻¹ | 0.088 mm ⁻¹ |
| $F(000)$ | 712 | 736 |
| <i>Data collection</i> | | |
| Diffractometer | X'calibur system (Oxford Diffraction make, U.K.) | X'calibur system (Oxford Diffraction make, U.K.) |
| Absorption correction | Multi-scan (CrysAlis RED; Oxford Diffraction, 2010) | Multi-scan (CrysAlis RED; Oxford Diffraction, 2010) |
| T_{\min} , T_{\max} | 0.89969, 1.00000 | 0.84990, 1.00000 |
| Reflections collected/unique | 4653/2506 | 7062/3497 |
| Reflections observed ($I > 2\sigma(I)$) | 1678 | 1448 |
| Scan mode | ω scan | ω scan |
| θ Range for entire data collection | 3.55° < θ < 26.00° | 3.57° < θ < 26.00° |
| Range of indices | $h = -17$ to 7 $k = -13$ to 10 $l = -10$ to 14 | $h = -15$ to 16 $k = -15$ to 9 $l = -12$ to 13 |
| Reflections collected/unique | 4653/2506 | 7062/3497 |
| Reflections observed ($I > 2\sigma(I)$) | 1678 | 1448 |
| R_{int} | 0.0232 | 0.0468 |
| R_{sigma} | 0.0411 | 0.1061 |
| <i>Refinement</i> | | |
| Refinement | Full-matrix least squares on F^2 | Full-matrix least squares on F^2 |
| No. of parameters refined | 226 | 244 |
| No. of restraints | 0 | 0 |
| $R[F^2 > 2\sigma(F^2)]$ | 0.0468 | 0.0486 |
| $wR(F^2)$ | 0.0913 | 0.0751 |
| Goodness-of-fit S | 1.045 | 0.878 |
| $(\Delta/\sigma)_{\text{max}}$ | 0.001 (for z C5) | 0.004 (for U ³³ C17) |
| Final residual electron density | -0.234 < $\Delta\rho$ < 0.123 e Å ⁻³ | -0.147 < $\Delta\rho$ < 0.136 e Å ⁻³ |
| Software for refinement | SHELXL97 [Sheldrick, 2008] | SHELXL97 [Sheldrick, 2008] |

separation energy; dispersion terms are simulated in London's inverse sixth power approximation, involving ionization potentials and polarizabilities; repulsion is presented as a

modulated function of wavefunction overlap. All the stabilizing molecular pairs involved in crystal packing were selected from the mlc output file, which is generated after PIXEL

Table 2. Geometry of C–H...O and C–H... π hydrogen bonds.

| D–H...A | D–H (Å) | D...A (Å) | H...A (Å) | D–H...A (°) |
|--|---------|-----------|-----------|-------------|
| I | | | | |
| C5–H5...O1 ⁱ | 0.93 | 2.55 | 3.392(3) | 150 |
| C7–H7...O1 ⁱ | 0.97 | 2.43 | 3.305(4) | 156 |
| C8–H8...Cg1 ⁱⁱ | 0.93 | 3.28 | 3.964(4) | 132 |
| C15–H15...Cg2 ⁱⁱⁱ | 0.93 | 3.09 | 3.983(4) | 161 |
| Symmetry code: (i) $x, -y-1/2, z-1/2$, (ii) $x, -y+1/2, z-1/2$ and (iii) $-x+1, y+1/2, -z+3/2$ | | | | |
| II | | | | |
| C2–H2...O3 ⁱ | 0.93 | 2.50 | 3.361(3) | 153 |
| C5–H5...O1 ⁱⁱ | 0.93 | 2.57 | 3.400(3) | 149 |
| C7–H7...O1 ⁱⁱ | 0.93 | 2.40 | 3.273(3) | 157 |
| C13–H13...Cg1 ⁱⁱⁱ | 0.93 | 2.95 | 3.754(3) | 145 |
| C8–H8...Cg2 ^{iv} | 0.93 | 3.12 | 3.949(3) | 150 |
| Symmetry code: (i) $x, -y+3/2, z+1/2$, (ii) $x, -y+1/2, z+1/2$ and (iii) $-x, -y+2, -z$ and (iv) $x, -y+3/2, z+1/2$ | | | | |

In **I**, Cg1 and Cg2 represent the centre of gravity of phenyl rings C11–C16 and C18–C23, respectively.

In **II**, Cg1 and Cg2 represent the centre of gravity of nitrophenyl ring and phenyl ring C18–C23, respectively.

Table 3. Geometry of π – π interactions. CgI...CgJ represent the distance between the ring centroids; CgI...P, the perpendicular distance of the centroid of one ring from the plane of the other; α is the dihedral angle between the planes of rings I and J; β is the angle between normal to the centroid of ring I and the line joining ring centroids; Δ is the displacement of the centroid of ring J relative to the intersection point of the normal to the centroid of ring I and the least-square plane of ring J.

| | CgI...CgJ (Å) | CgI...P (Å) | α (°) | β (°) | Δ (Å) |
|---|---------------|-------------|--------------|-------------|--------------|
| I | | | | | |
| Cg3...Cg3 ^{iv} | 3.955(2) | 3.480 | 0.00 | 28.39 | 1.87 |
| Cg4...Cg4 ^v | 3.891(2) | 3.479 | 0.02 | 26.60 | 1.74 |
| Cg1...Cg2 ^v | 3.857(2) | 3.402 | 2.79 | 25.33 | 1.81 |
| Symmetry code: (iv) $-x, -y, -z+1$ and (v) $-x+1, -y+1, -z+1$ | | | | | |
| II | | | | | |
| Cg1...Cg1 ^{iv} | 3.824(2) | 3.444 | 0.00 | 25.76 | 1.66 |
| Cg4...Cg4 ^v | 3.761(2) | 3.512 | 0.00 | 20.98 | 1.34 |
| Cg3...Cg2 ^v | 3.782(2) | 3.517 | 1.50 | 20.34 | 1.39 |
| Symmetry code: (iv) $-x, -y, -z+1$ and (v) $-x+1, -y+1, -z+1$ | | | | | |

In **I**, Cg1 and Cg2 represent the centre of gravity of phenyl rings C11–C16 and C18–C23, respectively, whereas Cg3 represents the centre of gravity of chlorophenyl ring and Cg4 represents the centre of gravity of phenyl ring (C10/C11/C16/C17/C18/C23).

In **II**, Cg1 represents the centre of gravity of nitrophenyl ring; Cg2 represents the centre of gravity of ring C18–C23; Cg3 represents the centre of gravity of C11–C16 ring and Cg4 represents the centre of gravity of C10/C11/C16/C17/C18/C23 ring.

energy calculations, and were analysed with their interaction energies. The symmetry operator and centroid–centroid distance along with coulombic, polarization, dispersion, repulsion and total interaction energies between the molecular pairs

are presented in table 4. The values of lattice energy for both the compounds are presented in table 5. The molecular pairs are arranged in decreasing order of their stabilization energies. The PIXEL method has been preferred for the

Table 4. Significant interaction energies (kcal mol⁻¹) between molecular pairs related by a symmetry operation and the associated intermolecular interactions in both the compounds.

| Motif | Centroid distance (Å) | E_{coul} | E_{pol} | E_{disp} | E_{rep} | E_{tot} | Symmetry | Important interactions |
|--------------------|-----------------------|-------------------|------------------|-------------------|------------------|------------------|-----------------------|--|
| Compound I | | | | | | | | |
| 1 | 9.477 | -3.22 | -1.60 | -14.84 | 8.58 | -11.06 | $-1-x, -1-y, 1-z$ | $\pi-\pi$ |
| 2 | 5.924 | -3.82 | -2.46 | -11.64 | 7.43 | -10.47 | $x, -1/2-y, -1/2+z$ | C5-H5...O1 C7-H7...O1 |
| 3 | 9.240 | -2.22 | -0.86 | -11.26 | 6.14 | -8.19 | $-x, -y, 1-z$ | C12...C11 C13...C11 |
| 4 | 7.445 | -1.36 | -0.84 | -8.00 | 4.06 | -6.14 | $-1-x, -y, 1-z$ | C20-H20...C1 C21-H21...C6 C21-H21...C7 |
| 5 | 8.919 | -1.38 | -0.84 | -6.09 | 3.77 | -4.54 | $-1-x, -1/2+y, 1/2-z$ | C19-H19...Cg3 C15-H15...Cg2 |
| 6 | 9.542 | -0.23 | -0.47 | -4.61 | 1.84 | -3.51 | $-x, -1/2+y, 3/2-z$ | C12-H12...C2 C8-H8...C11 |
| 7 | 11.079 | -0.93 | -0.50 | -4.06 | 2.44 | -3.08 | $x, -1+y, z$ | C13-H13...C11 C14-H14...C11 |
| 8 | 11.111 | -0.86 | -0.26 | -2.34 | 0.91 | -2.58 | $x, 1/2-y, 1/2+z$ | C2-H2...C11 |
| Compound II | | | | | | | | |
| 1 | 5.743 | -4.85 | -2.60 | -12.71 | 8.03 | -12.14 | $x, 1/2-y, 1/2+z$ | C5-H5...O1 C7-H7...O1 |
| 2 | 9.723 | -2.74 | -1.36 | -14.43 | 7.00 | -11.54 | $2-x, -y, 1-z$ | $\pi-\pi$ |
| 3 | 8.983 | -1.15 | -0.98 | -9.63 | 4.51 | -7.24 | $1-x, 1-y, 1-z$ | $\pi-\pi$ O3...C6 O3...C7 |
| 4 | 7.391 | -0.79 | -0.67 | -7.38 | 3.66 | -5.18 | $2-x, 1-y, 1-z$ | C14-H14...C2 C13-H13...Cg1 |
| 5 | 9.450 | -1.05 | -0.76 | -5.69 | 3.13 | -4.37 | $2-x, 1/2+y, 3/2-z$ | C15-H15...Cg1 C19-H19...Cg3 |
| 6 | 10.112 | -1.09 | -0.57 | -3.85 | 1.58 | -3.94 | $1-x, -1/2+y, 1/2-z$ | C8-H8...O2 |

Table 5. PIXELC lattice energy calculation output (kcal mol⁻¹).

| | E_{coul} | E_{pol} | E_{disp} | E_{rep} | E_{tot} |
|-------------|-------------------|------------------|-------------------|------------------|------------------|
| Compound I | -11.02 | -6.12 | -47.75 | 25.81 | -39.08 |
| Compound II | -11.61 | -5.62 | -43.76 | 22.87 | -38.12 |

quantification of intermolecular interactions, primarily because of the following reasons:

- (1) it is computationally less demanding [23];
- (2) it allows partitioning of total interaction energy into corresponding coulombic, polarization, dispersion and repulsion contribution, which facilitates a better understanding of the nature of intermolecular interactions contributing towards the crystal packing [24];

- (3) the energies obtained from PIXEL calculation are generally comparable with high-level quantum mechanical calculations [25,26].

4. Results and discussion

ORTEP diagrams of the compounds were generated using ORTEP32 [27] and packing diagram was generated using PLATON [21] software. Both the compounds crystallize in the monoclinic crystal system with space group P2₁/c. The bond distances of compounds I and II show normal values [28] and are comparable with those observed in related structures [14–17].

The molecular structure of I is shown in figure 1. In title compound I, C₂₃H₁₅Cl₁O₁, the prop-2-en-1-one unit is planar

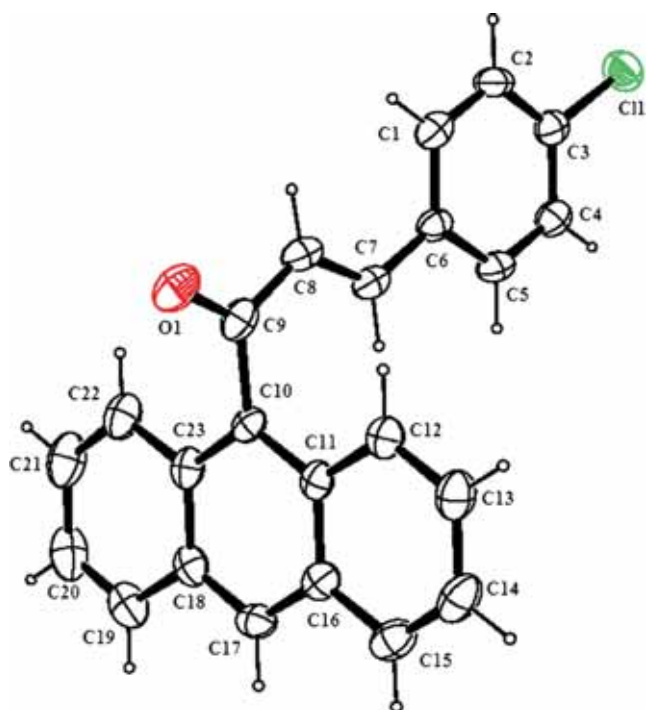


Figure 1. Molecular structure of **I**, showing the atomic labelling scheme. Displacement ellipsoids are drawn at 30% probability level.

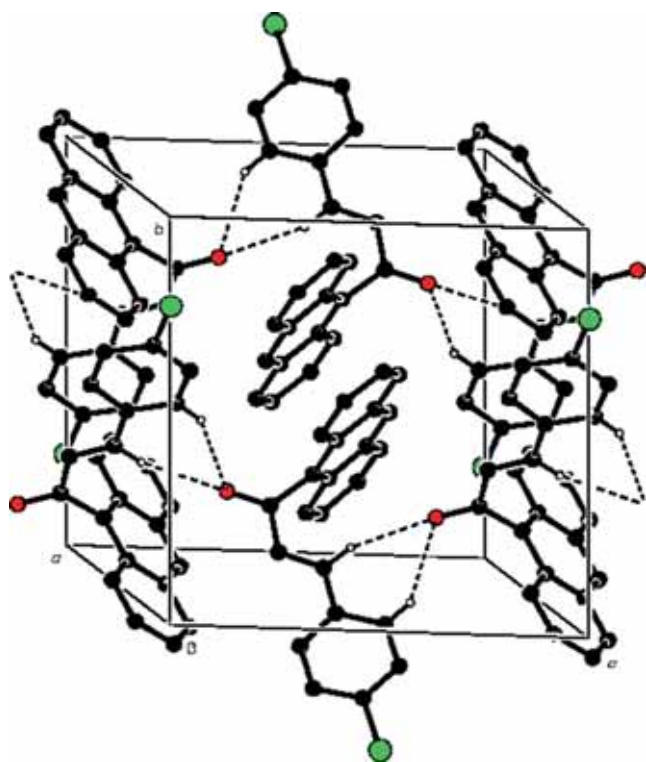


Figure 2. Crystal packing of compound **I**, viewed along the *a* axis, showing hydrogen bonding (dashed lines).

and it makes dihedral angles of $1.52(15)^\circ$ and $80.52(17)^\circ$, respectively, with the 4-chlorophenyl ring and the anthracene ring system. In compound **I**, the anthracene ring system is planar and the molecule is twisted as indicated by the interplanar angle between the 4-chlorophenyl ring and the anthracene ring system, which is $79.32(6)^\circ$. The pro-2-en-1-one unit (C7–C9/O1) is planar as evidenced by the torsion angle O1–C9–C8–C7 of $174.8(3)^\circ$. The length of the double bond C9 = O1 is confirmed by the respective distance of $1.228(3) \text{ \AA}$. Molecule **I** adopts a *trans(-)gauche-trans* (tgt) conformation [torsion angles ($^\circ$): C6–C7–C8–C9, $-178.4(2)^\circ$; C7–C8–C9–C10, $-4.8(4)^\circ$; C7–C8–C9–O1, $174.8(3)^\circ$]. In this crystal, adjacent molecules are interconnected through C–H...O hydrogen bonds shown in figure 2. The crystal structure is further stabilized by C–H... π hydrogen bonding and π – π interactions.

Molecular pairs of the compound **I** extracted from crystal structure along with their respective interaction energies are shown in figure 3. The maximum stabilization to the crystal structure comes from π – π interaction between anthracene ring systems. The stabilization energy of this pair is $-11.06 \text{ kcal mol}^{-1}$ obtained using PIXEL with major contribution from dispersion component. The next most stabilized pair (Motif 2) shows the presence of bifurcated acceptor atom O1 with H5 and H7 having interaction energy of $-10.47 \text{ kcal mol}^{-1}$. The next most stabilized pair (Motif 3) involves C12...C11 and C13...C11 interactions. Along with these interactions it also involves in molecular stacking (C–C stacking) and hence results in a total interaction energy of $-8.19 \text{ kcal mol}^{-1}$. The next molecular pair (Motif 4) shows the presence of C–H...C interaction involving H20 interacting with C1 and bifurcated donor atom C21 interacting with C6 and C7, generating dimers with stabilization energy of $-6.14 \text{ kcal mol}^{-1}$. The maximum stabilization to the next molecular pair (Motif 5) comes from C–H... π intermolecular interactions involving H19 with C4 and C5 of Cg1 [where Cg1 is the centroid of benzene ring (C1–C6)] and H15 interacting with Cg4 [where Cg4 is the centroid of benzene ring (C18–C23)]. The stabilization energy of this pair is $-4.54 \text{ kcal mol}^{-1}$ obtained using PIXEL. Molecular pair 6 shows the presence of C–H...C (involving H12 with C2) and C–H...Cl interaction (involving H8 with Cl1), resulting in a stabilization energy of $-3.51 \text{ kcal mol}^{-1}$. Another molecular pair (Motif 7) shows the presence of bifurcated acceptor atom Cl1 interacting with H13 and H14 having interaction energy of $-3.08 \text{ kcal mol}^{-1}$ with major contribution from dispersion component. The next most stabilized molecular pair (Motif 8) again involves in C–H...Cl hydrogen bonding involving H2 interacting with Cl1 with an interaction energy of $-2.58 \text{ kcal mol}^{-1}$ and the stabilization mainly comes from dispersion component, providing additional stabilization to the crystal packing. The combined nature of all these interactions is mainly dispersive in nature.

The molecular structure of **II** is shown in figure 4. In title compound **II**, $\text{C}_{23}\text{H}_{15}\text{N}_1\text{O}_3$, the prop-2-en-1-one unit is

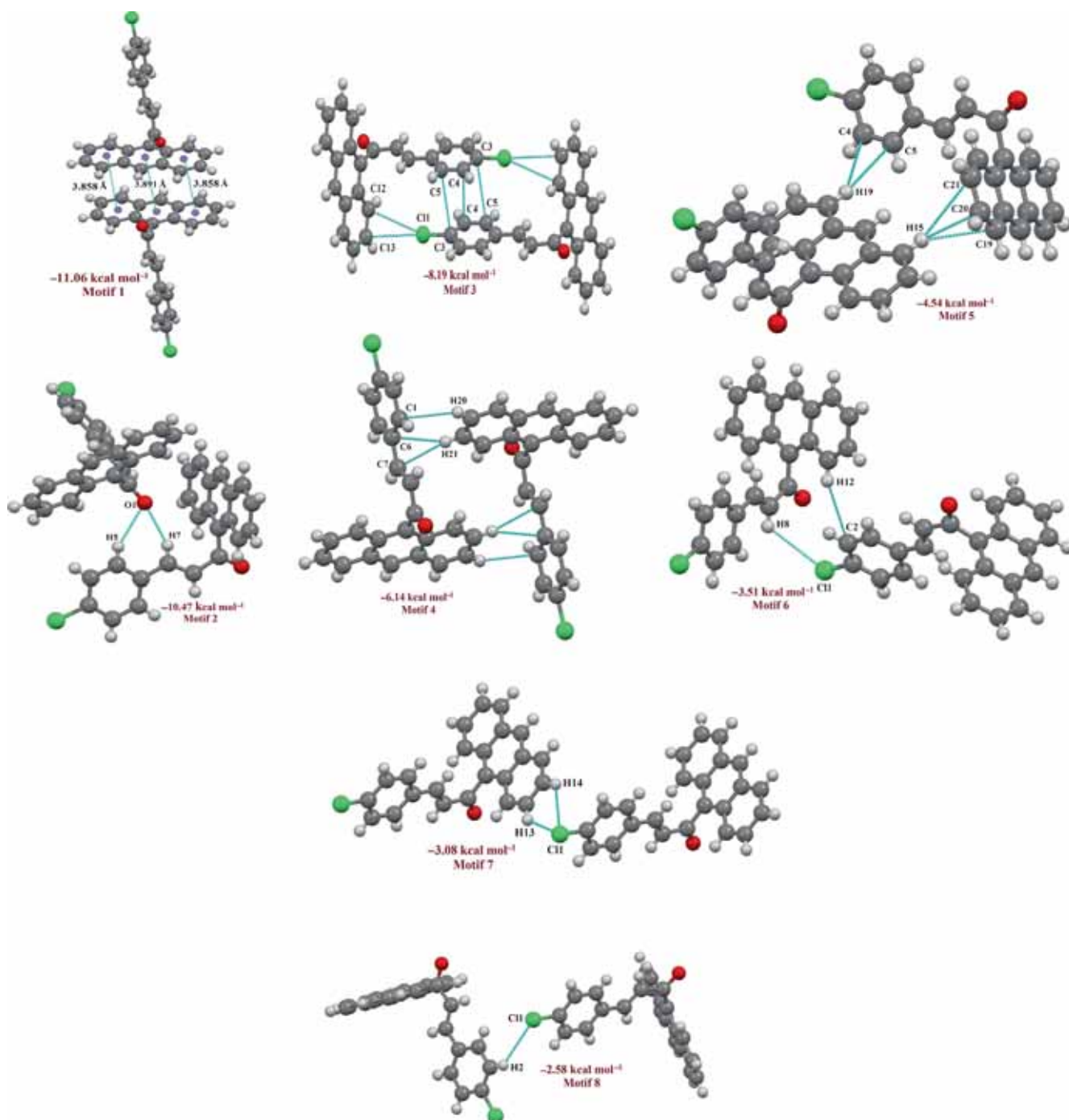


Figure 3. Molecular pairs (1–8) with their interaction energies for compound **I**.

also planar and it makes dihedral angles of $7.30(23)^\circ$ and $86.96(17)^\circ$, respectively, with the 4-nitrophenyl ring and the anthracene ring system. In this compound the anthracene ring system is planar and the molecule is twisted as indicated by the interplanar angle between the 4-nitrophenyl ring and the anthracene ring system, which is $88.87(6)^\circ$. The pro-2-en-1-one unit (C7–C9/O1) is planar as evidenced by the torsion angle O1–C9–C8–C7 of $177.9(2)^\circ$. The O–N–O

angle in the NO₂ group is significantly greater than 120° as a result of the lone pair of electrons on each of the O atoms; this effect is predicted by the valence-shell electron-pair repulsion theory [29,30]. The length of the double bond C9=O1 is confirmed by the respective distance of $1.223(2)$ Å. Molecule **II** adopts a *trans(-)gauche-trans* (tgt) conformation [torsion angles ($^\circ$): C6–C7–C8–C9, $-178.7(2)$; C7–C8–C9–C10, $-2.6(4)$; C7–C8–C9–O1, $177.9(2)$]. Three

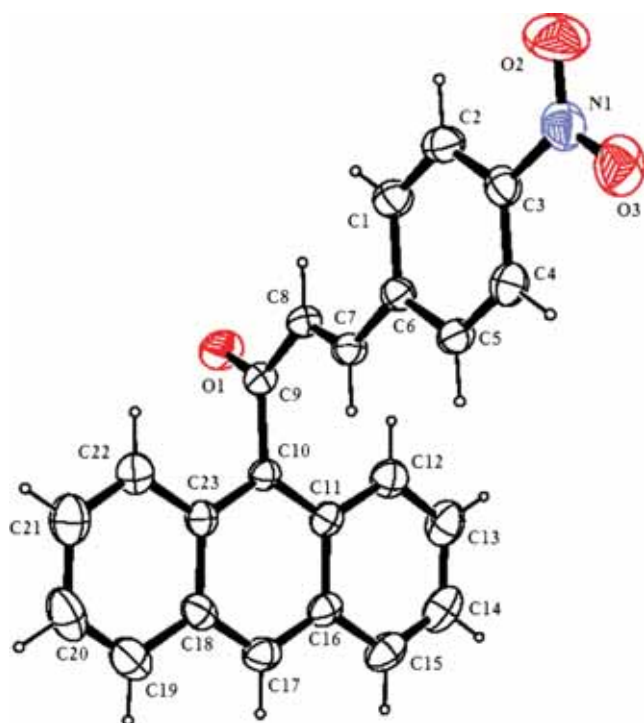


Figure 4. Molecular structure of **II**, showing the atomic labelling scheme. Displacement ellipsoids are drawn at 30% probability level.

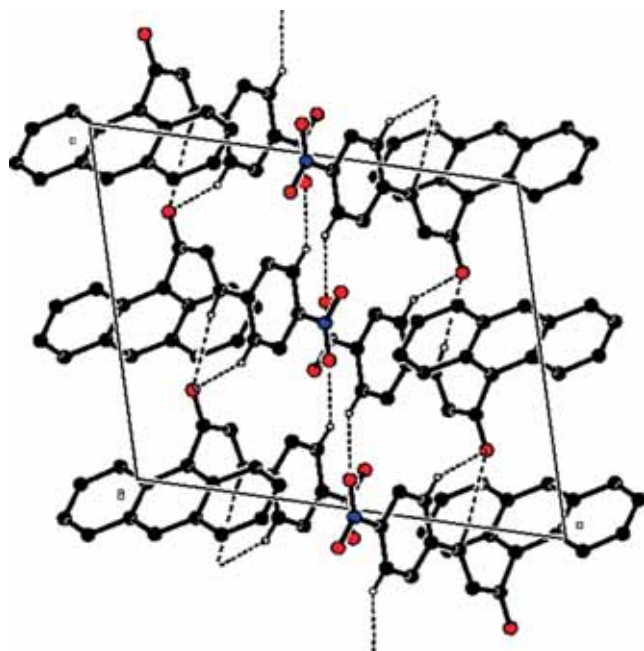


Figure 5. Crystal packing of compound **II**, viewed along the *a* axis, showing hydrogen bonding (dashed lines).

C–H...O inter molecular hydrogen bond interactions are observed. These intermolecular interactions are responsible

for maintaining the crystal packing. The crystal structure is further stabilized by C–H... π and π ... π interactions shown in figure 5.

Molecular pairs of compound **II** extracted from its crystal structure along with their respective interaction energies are shown in figure 6. The maximum stabilization to the crystal structure comes from C–H...O interaction involving bifurcated acceptor atom O1 with H5 and H7 having interaction energy of $-12.14 \text{ kcal mol}^{-1}$. The molecular pair (Motif 1) in this compound **II** is similar to the most stabilized motif (Motif 2) in compound **I**. The next most stabilized pair (Motif 2) in this compound **II** is also similar to the most stabilized Motif 1 in compound **I**, resulting in a stabilization energy of $-11.54 \text{ kcal mol}^{-1}$. The third most stabilized interacting motif (Motif 3) shows the presence of C6...O3 and C7...O3 interactions. Along with these interactions it also involves in π – π interactions, resulting in a total interaction energy of $-7.24 \text{ kcal mol}^{-1}$. The next molecular pair (Motif 4) shows the presence of C–H... π and C–H...C interaction involving H13 interacting with Cg1 [where Cg1 is the centroid of benzene ring (C1–C6)] and H14 interacting with C2, generating dimers and resulting in a stabilization energy of $-5.18 \text{ kcal mol}^{-1}$. The maximum stabilization to the next molecular pair (Motif 5) comes from C–H... π intermolecular interactions involving H19 with C13 and C14 of Cg3 [where Cg3 is the centroid of benzene ring (C11–C16)] and H15 interacting with Cg1 [where Cg1 is the centroid of benzene ring (C1–C6)]. The stabilization energy of this pair is $-4.37 \text{ kcal mol}^{-1}$ obtained using PIXEL. Molecular pair 6 shows the presence of C–H...O (involving H8 with O2) interaction resulting in a stabilization energy of $-3.94 \text{ kcal mol}^{-1}$. The combined nature of all these interactions in compound **II** is mainly dispersive in nature again.

5. Conclusions

The molecular and crystal structure of chalcone derivatives has been elucidated by X-ray diffraction methods and the results show the presence of different key structural motifs, which aid stabilization of crystal packing in the unit cell. The total interaction energy (lattice energy) appears to be the same for both the compounds [$-39.08 \text{ kcal mol}^{-1}$ for compound **I** and $-38.12 \text{ kcal mol}^{-1}$ for compound **II**]. The present study can help us in designing different biologically active derivatives of chalcone by changing the strength of donor and/or acceptor atom, which can give rise to interactions of different strength and nature, which in turn can help in identifying binding capabilities of such molecules with enzymes. In summary, the results demonstrated that the calculation of lattice energies is a useful approach to assess the stability of molecular crystals in which dispersion-type interactions make up an essential part of the intermolecular interactions.

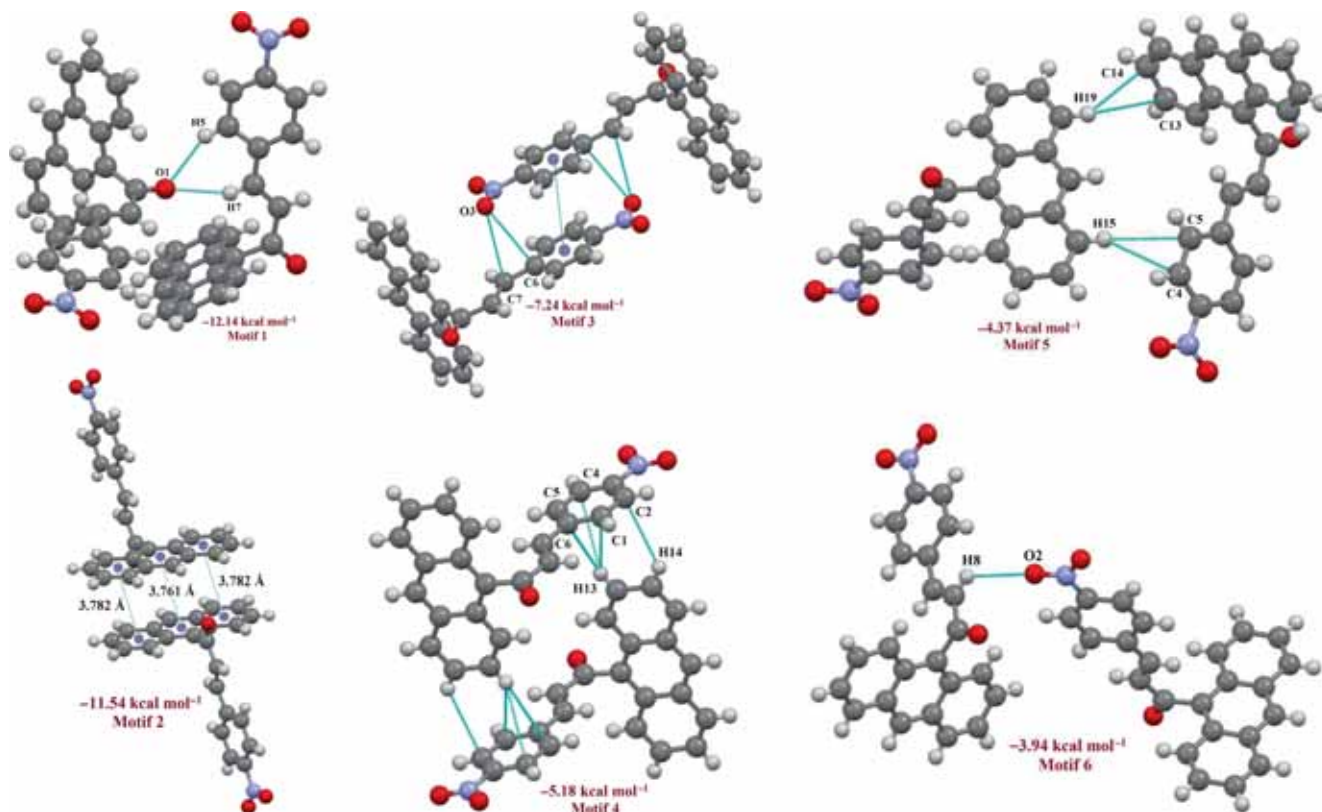


Figure 6. Molecular pairs (1–6) with their interaction energies for compound II.

Acknowledgements

RK acknowledges the Department of Science and Technology for the Single-Crystal X-ray Diffractometer sanctioned as a National Facility under Project No. SR/S2/CMP-47/2003. BN thanks UGC for financial assistance through BSR one-time grant for the purchase of chemicals. VVS thanks Mangalore University for research facilities.

References

- [1] Wong E 1968 *Phytochemistry* **7** 1751
- [2] Belofsky G, Percivill D, Lewis K, Tegos G P and Ekart J 2004 *J. Nat. Prod.* **67** 481
- [3] Nielsen S F, Christensen S B, Cruciani G, Kharazmi A and Liljefors T 1998 *J. Med. Chem.* **41** 4819
- [4] Wang L, Chen G, Lu X, Wang S, Han S, Li Y, Ping G, Jiang X, Li H, Yang J and Wu C 2015 *Eur. J. Med. Chem.* **89** 88
- [5] Dimmock J R, Elias D W, Beazely M A and Kandepu N M 1999 *Curr. Med. Chem.* **6** 1125
- [6] Lopez S N, Castelli M V, Zacchino S A, Dominguez J N, Lobo G, Jaime C C, Cortes J C G, Ribas J C, Devia C, Ana M R and Ricardo D E 2001 *Bioorg. Med. Chem.* **9** 1999
- [7] Agarwal A, Srivastava K, Puri S K and Chauhan P M S 2005 *Bioorg. Med. Chem.* **13** 4645
- [8] Kumar D, Kuma N M, Tantak M P, Ogura M, Kusaka E and Ito T 2014 *Bioorg. Med. Chem.* **24** 5170
- [9] Fang Q, Zhao L, Wang Y, Zhang Y, Li Z, Pan Y, Kanchana K, Wang J, Tong C, Li D and Liang G 2015 *Toxicol. Appl. Pharm.* **282** 129
- [10] Samshuddin S, Narayana B, Shetty D N and Raghavendra R 2011 *Der. Pharma. Chem.* **3** 232
- [11] Baktir Z, Akkrut M, Samshuddin S, Narayana B and Yathirajan H S 2011 *Acta Crystallogr. E* **67** o1292
- [12] Sapnakumari M, Narayana B, Sarojini B K and Madhu L N 2014 *Med. Chem. Res.* **23** 2368
- [13] Poornesh P, Shettigar S, Umesh G, Manjunatha K B, Kamath K P, Sarojini B K and Narayana B 2009 *Opt. Mater.* **31** 854
- [14] Jasinski J P, Guild C J, Samshuddin S, Narayana B and Yathirajan H S 2010 *Acta Crystallogr. E* **66** o2018
- [15] Butcher R J, Yathirajan H S, Anilkumar H G, Sarojini B K and Narayana B 2006 *Acta Crystallogr. E* **62** o1633
- [16] Narayana B, Salián V V, Sarojini B K and Jasinski J P 2014 *Acta Crystallogr. E* **70** o855
- [17] Harrison W T A, Yathirajan H S, Sarojini B K, Narayana B and Vijay Raj K K 2006 *Acta Crystallogr. E* **62** o1578
- [18] Oxford Diffraction 2010 *CrysAlis PRO* (Yarnton, England: Oxford Diffraction Ltd)
- [19] Sheldrick G M 2008 *Acta Crystallogr. A* **64** 112
- [20] Farrugia L J 1999 *J. Appl. Crystallogr.* **32** 837
- [21] Spek A L 2009 *Acta Crystallogr. D* **65** 148

- [22] Nardelli M 1995 *J. Appl. Crystallogr.* **28** 659
- [23] Gavezzotti A 2011 *New J. Chem.* **35** 1360
- [24] Dunitz J D and Gavezzotti A 2012 *Cryst. Growth Des.* **12** 5873
- [25] Maschio L, Civalleri B, Ugliengo P and Gavezzotti A 2011 *J. Phys. Chem. A* **115** 11179
- [26] Dunitz J D and Gavezzotti A 2005 *Chem. Soc. Rev.* **38** 2622
- [27] Farrugia L J 2012 *J. Appl. Crystallogr.* **45** 849
- [28] Allen F H, Kennard O, Watson D G, Brammer L, Prpen A G and Taylor R 1987 *J. Chem. Soc. Perkin Trans.* **2** S1
- [29] Gillespie R J 1963 *J. Chem. Educ.* **40** 295
- [30] Gillespie R J 1992 *Chem. Soc. Rev.* **21** 59